Key issues for long-pulse high-$_N$ operation with the *Experimental Advanced Superconducting Tokamak* (EAST)

2017 Nucl. Fusion 57 056021

(http://iopscience.iop.org/0029-5515/57/5/056021)

OPEN ACCESS
IOP Publishing | International Atomic Energy Agency
Nuclear Fusion
Nucl. Fusion **57** (2017) 056021 (8pp)
https://doi.org/10.1088/1741-4326/aa626c

Key issues for long-pulse high-β_N operation with the *Experimental Advanced Superconducting Tokamak* (EAST)

Xiang Gao[1], Yao Yang[1], Tao Zhang[1], Haiqing Liu[1], Guoqiang Li[1], Tingfeng Ming[1], Zixi Liu[1], Yumin Wang[1], Long Zeng[1], Xiang Han[1], Yukai Liu[1], Muquan Wu[1], Hao Qu[1], Biao Shen[1], Qing Zang[1], Yaowei Yu[1], Defeng Kong[1], Wei Gao[1], Ling Zhang[1], Huishan Cai[2], Xuemei Wu[3], K. Hanada[4], Fubin Zhong[1], Yunfeng Liang[1], Chundong Hu[1], Fukun Liu[1], Xianzhu Gong[1], Bingjia Xiao[1], Baonian Wan[1], Xiaodong Zhang[1], Jiangang Li[1] and the EAST Team[1]

[1] Institute of Plasma Physics, Chinese Academy of Sciences, PO Box 1126, Hefei, Anhui 230031, People's Republic of China
[2] Department of Modern Physics, University of Science and Technology of China, Hefei, Anhui 230026, People's Republic of China
[3] College of Physics, Soochow University, Suzhou 215006, People's Republic of China
[4] Research Institute for Applied Mechanics, Kyushu University, Kasuga, Fukuoka, Japan

E-mail: xgao@ipp.ac.cn

Received 15 December 2016, revised 15 February 2017
Accepted for publication 23 February 2017
Published 24 March 2017

Abstract

In the last few years, long-pulse H-mode plasma discharges (with small edge-localized modes and normalized beta, $\beta_N \sim 1$) have been realized at the *Experimental Advanced Superconducting Tokamak* (EAST). This paper reports on high-β_N (>1.5) discharges in the 2015 EAST campaign. The characteristics of these H-mode plasmas have been presented in a database. Analysis of the experimental limit of β_N has revealed several main features of typical discharges. Firstly, efficient, stable high heating power is required. Secondly, control of impurity radiation (partly due to interaction between the plasma and the in-vessel components) is also a critical issue for the maintenance of high-β_N discharges. In addition an internal transport barrier (ITB) has recently been observed in EAST, introducing further improvement in confinement surpassing H-mode plasmas. ITB dynamics is another key issue for high-β_N plasmas in EAST. Each of these features is discussed in this paper. Study and improvement of these issues could be considered as the key to achieving long-pulse high-β_N operation with EAST.

Keywords: H mode, high normalized beta, long pulse

(Some figures may appear in colour only in the online journal)

1. Introduction

One important goal of ITER is to demonstrate steady-state tokamak operation on a reactor scale [1]. Steady-state operation means sustaining the toroidal plasma current by a combination of just the external current drive scheme (like neutral beam injection (NBI) and radiofrequency (RF) waves) and the bootstrap current driven by the local pressure gradient. While ITER operates for ~400 s with the baseline scenario or the inductive scenario, the ITER steady-state scenario will demonstrate full non-inductive current drive and have a pulse length of 3000 s [2]. The ITER hybrid scenario

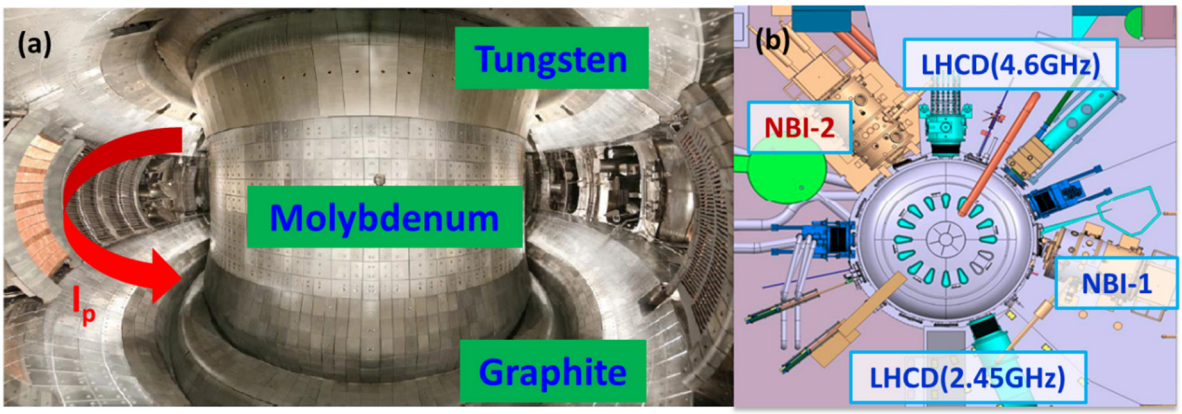

Figure 1. Experimental setup for high-β_N discharges in the 2015 EAST campaign. (*a*) EAST vacuum vessel and plasma current direction. The three main in-vessel materials are molybdenum for the first wall, graphite for the lower divertor plate and tungsten for the upper divertor plate. (*b*) Main heating and current driving systems for this study: LHW and NBI.

is an intermediate step between the inductive scenario and the steady-state scenario. Meanwhile, the fusion gain is proportional to normalized beta (β_N) with certain conditions [3]. This indicates that high-β_N operation is desirable for steady-state operation.

Starting from the ITER baseline scenario, different types of advanced scenarios have been developed and studied by fusion scientists. Current studies indicate three main categories of advanced scenario in present-day tokamaks [2]. The first includes scenarios with a moderate safety factor, q profile and a center q value between 1.5 and 2.5. These discharges (JT-60U [4–6], DIII-D [7–9], JET [10]) are considered as good candidates for ITER steady-state operation. The second category contains high-bootstrap-fraction plasmas with strongly reversed shear. These examples can be beneficial for the study of steady-state operation but several issues need to be resolved before they are attractive for ITER. References to this category can be found in [11–14]. The third category refers to those scenarios with low or even no shear and a center q value around 1. Studies on this subject have been carried out in different machines (JT-60U [15], ASDEX-U [16, 17], DIII-D [18, 19]). These discharges are good candidates for the hybrid scenario.

The *Experimental Advanced Superconducting Tokamak* (EAST) established a 32 s (about 20 current diffusion times) H mode in the 2012 campaign [20]. Those discharges were conducted with small edge-localized modes (ELMs) and low β_N (~1) due to limited external power from lower hybrid wave (LHW) and ion cyclotron resonance heating (ICRH). Since then the heating and current drive system have been significantly improved on EAST. New neutral beam injection (NBI) heating and electron cyclotron resonance heating (ECRH) systems have been developed. LHW and ICRH systems have been upgraded. Another long-pulse H-mode discharge (longer than 60 s, $\beta_N \sim 1$) has been reported recently [21].

In order to explore a confinement regime with longer pulse duration, the work in this paper considers the development of a higher β_N (~2) scenario on EAST. Based on the newly upgraded heating and current drive systems, a long-pulse scenario with higher $\beta_N \sim 2$ was predicted using simulation tools [22]. In the 2015 EAST campaign, reproducible discharges with $\beta_N > 1.5$ were performed and are analyzed in this paper. Different experimental limits will be presented and discussed as key issues for long-pulse high-β_N operation on EAST.

2. Experimental setup for high-β_N discharges in EAST

In the 2015 EAST campaign, β_N was improved compared with the long-pulse H-mode plasmas previously achieved with EAST. This is mainly due to the upgrade of the heating and current drive systems. The new 4.6 GHz LHW system and new NBI (co- and counter-current directions) systems were proved to be reliable for routine EAST operation [23]. A set of higher-β_N discharges were obtained. The main plasma parameters for these discharges were plasma current (I_p) 300–500 kA, toroidal field (B_T) 1.7–2.2 T and electron density (n_e) (3–5) $\times$ 10^{19} m^{-3}. The main heating powers were LHW (3 MW) and NBI (2 MW for co- and counter-current beams, respectively). Other heating sources such as ECRH (0.4 MW) and ICRF (2 MW source power) were either low or inefficient. EAST was equipped with a molybdenum first wall, a graphite lower divertor and a tungsten upper divertor. In these discharges, the plasmas were in single null lower divertor configuration.

A database of discharges with $\beta_N > 1.5$ was obtained (48 shots in all). The operation space of this database is presented in figure 2. The heating power varied from 2 MW to 5.5 MW while the maximum β reached a value of around 2. The β_N values were estimated from real-time EFIT calculation. Each data point was taken from one single discharge when β_N reached its maximum value. Here, the heating powers (LHW, NBI, etc) in the total power were processed using a factor of 80% from the source power. The factors were also used to calculate the H factor on EAST in some cases. β_N increases with increasing heating power. This trend needs to be tested with higher heating powers. Additionally, those discharges with a toroidal field in the counter-current direction have higher β than in co-current direction B_T discharges. In the lower single null divertor configuration the toroidal field in the counter-I_p

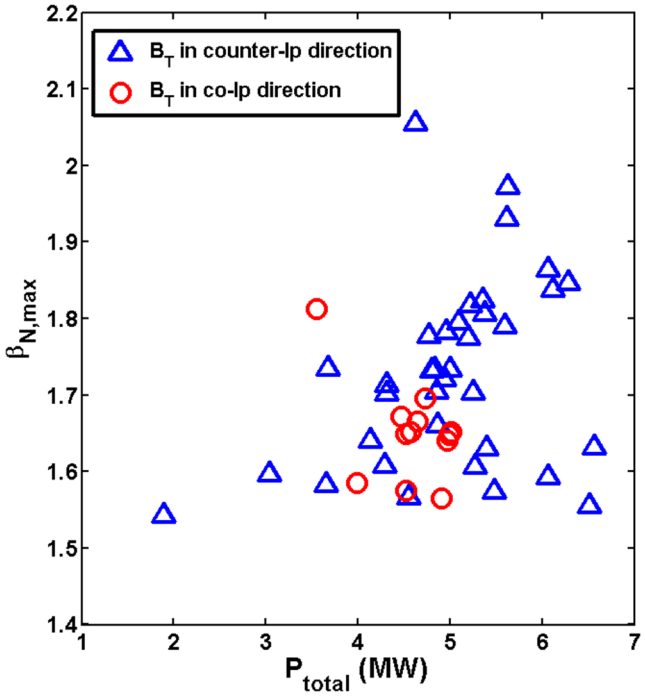

Figure 2. Operational space of high-β_N discharges in the 2015 EAST campaign.

direction is actually a favorable toroidal field since the plasma current is anti-clockwise in EAST.

3. High-β_N plasmas in EAST

3.1. High heating power is essential for high-β_N plasmas

The reliability of the heating power is an important requirement for achieving and maintaining a high-β_N plasma. Figure 3 gives an example of this. In this discharge, the plasma current was 480 kA and the toroidal field was about 1.7 T. The plasma density was 3×10^{19} m^{-3} (far-infrared interferometer measurement). The H mode was established by NBI injection at $t = 2.96$ s with a LHW background (0.9 MW at 2.45 GHz and 1.2 MW at 4.6 GHz). The ELMs are observed to be mitigated from $t = 3.5$ to $t = 4.8$ s due to application of resonant magnetic perturbation (RMP) coils. However, application of the RMP coils had little influence on the confinement, as shown in the plasma stored energy signal. The unperturbed ELM was restored at $t = 4.8$ s.

From $t = 3.5$ to $t = 5$ s β_N was sustained for 1.5 s. Following drop of the NBI power at $t = 5.25$ s, indicated as a black dotted line in figure 3, β_N clearly dropped below 1.5. In fact, for each NBI beam there are two sources of neutral beams (called left and right sources in EAST). This drop was caused by turning off one of the two sources for both NBIs. By decreasing the NBI power by nearly 50%, β_N dropped to 1.2 but the discharge remained in the H mode. A similar behavior can be observed for the plasma stored energy signal. The plasma transitioned back to L mode shortly after complete turn-off of the NBI power.

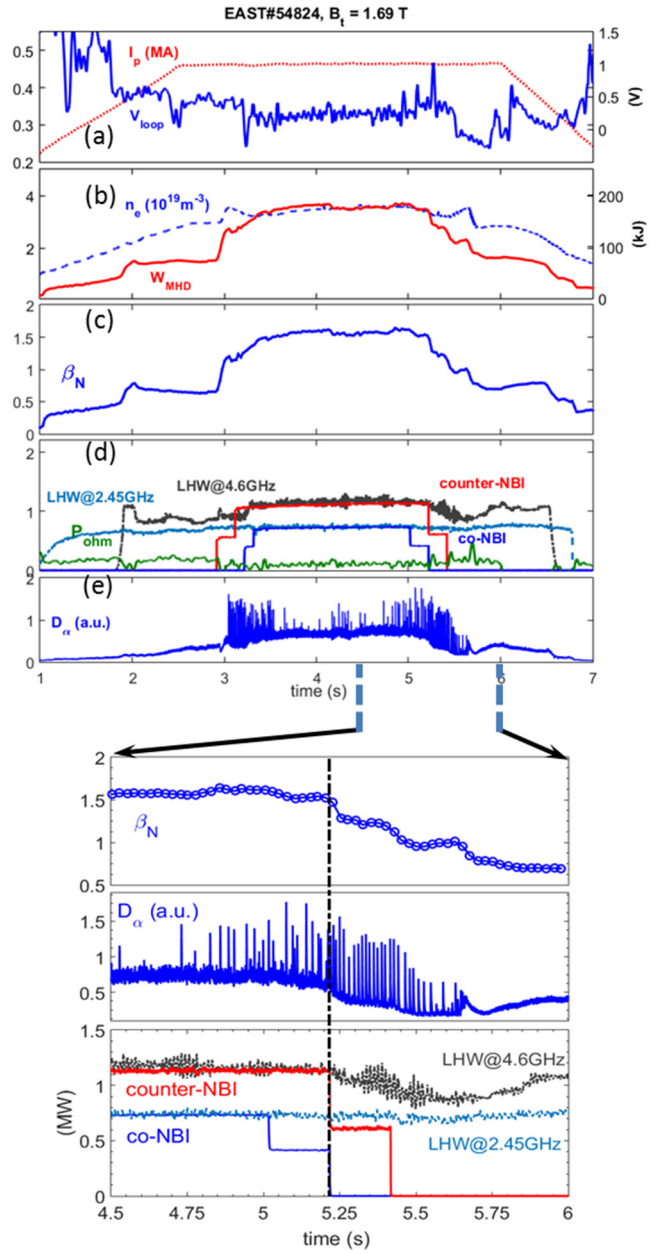

Figure 3. High-β_N limitation due to turn-off of the heating power. Time traces in the upper figure are (*a*) plasma and loop voltage, (*b*) plasma density and stored energy, (*c*) β_N, (*d*) external heating powers and ohmic power, (*e*) D_α signal indicating an ELM. The lower figure shows the time window between 4.5 s and 6 s in more detail, implying the dropout of β_N following the turning off of the heating power.

In the experiment, turning off of the heating power usually comes from the high-voltage breakdown of the NBI sources. About 35.5% (17 out of 48) of dropouts of the high-β_N phase are due to turn-off of the heating power (either partly or entirely). This indicates that in order to perform long-pulse high-β discharges in EAST, the increase and sustainment of the heating power system is a key requirement. On this aspect, EAST has been improved considerably since the 2015 campaign.

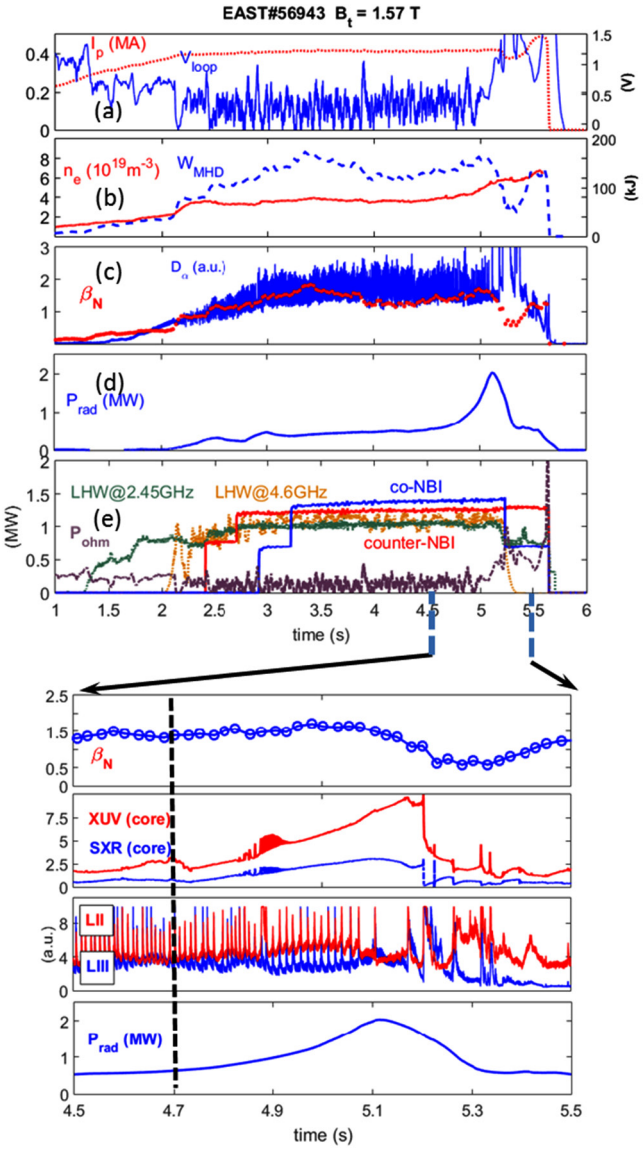

Figure 4. Impurity radiation issues with EAST. Time traces in the upper figure are (*a*) plasma current and loop voltage, (*b*) plasma density and stored energy, (*c*) β_N and D_α signal as an indication of ELM, (*d*) the total radiation power, (*e*) external heating powers and ohmic power. The lower figure shows the time window between 4.5 s and 5.5 s in more detail, implying the dropout of β_N associated with impurity activities.

3.2. Impurity control is an important issue for high-β_N operation

The transport of impurities and the associated control are further critical issues in the enhanced confinement regime and for the burning plasma. This is due to the core cooling effect and instabilities driven from the accumulation of impurities. Additionally, the accumulation of impurities can cause excessive fuel dilution in burning plasma. A number of methods to control impurities have been performed on various machines using ECRH [24] or ICRH [25].

A discharge from the EAST high-β_N database with strong impurity activity is shown in figure 4. The plasma current was 450 kA and the toroidal field 1.57 T. The plasma density was 3.5×10^{19} m^{-3}. The plasma entered H mode at $t = 2$ s

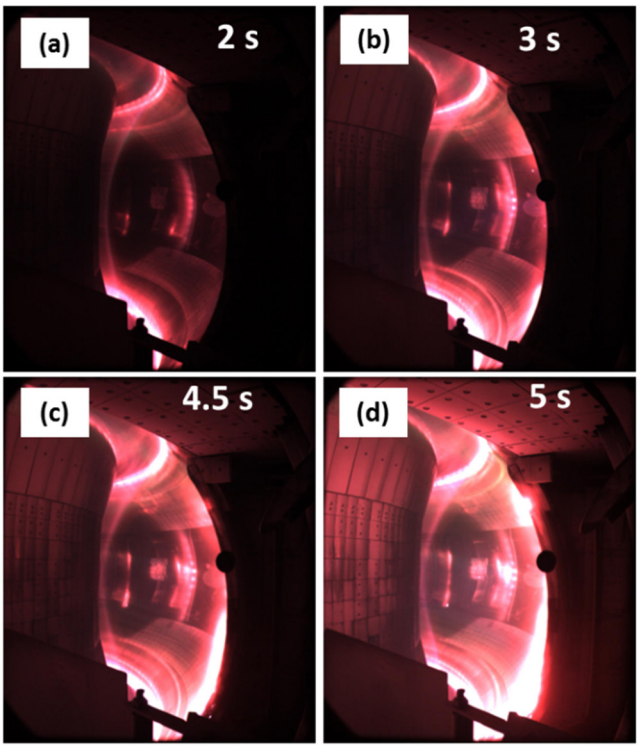

Figure 5. Fast camera images of EAST#56943, (*a*) $t = 2$ s, (*b*) $t = 3$ s, (*c*) $t = 4.5$ s, (*d*) $t = 5$ s, where (*c*) and (*d*) show impurity behaviors after $t = 4.5$ s.

by the injection of 4.6 GHz LHW (1.4 MW). Later on, two NBIs increased the plasma confinement further. β_N was maintained above 1.4. At $t = 4.7$ s, indicated by the black dotted line in the lower part of figure 4, the plasma radiated power (calculated from the XUV radiation signal) started to rise. As the radiation power increased, β_N was maintained until $t = 5.05$ s. Later, the radiation power reached its peak value ($t = 5.1$ s), leading to disruption of the plasma. During the increase in the radiation power the heating power remained unchanged. The NBI power started to shut down at $t = 5.25$ s when the plasma was already disrupted.

A fast CCD camera (visible wavelength) image is shown in figure 5. From $t = 4.5$ s (figure 5(*c*)) to $t = 5$ s (figure 5(*d*)) the heating power (LHW and NBI) remained constant, but frequent impurity spark-like events were observed. This means that the plasma edge touched the in-vessel components and there were strong plasma–material interactions. These events could bring in impurity species. Currently it is not quite clear what the main impurity source for the plasma is. One study showed a possible fast electron flux driven by LHW in the scrape-off layer (SOL) regime [26]. This flux could interact with the protecting limiter in front of the LHW antennae and introduce impurities into the plasma.

For further study of impurity behavior during impurity accumulation, the time evolution of impurity line intensity was measured by a fast-response EUV spectrometer on EAST (see figure 6). It was found that the density of heavy impurities, e.g. iron and tungsten, increased quickly from 4.85 s to 5.2 s. As the impurities accumulated until $t = 5.1$ s, H–L back transition appeared and led to further disruption. In the

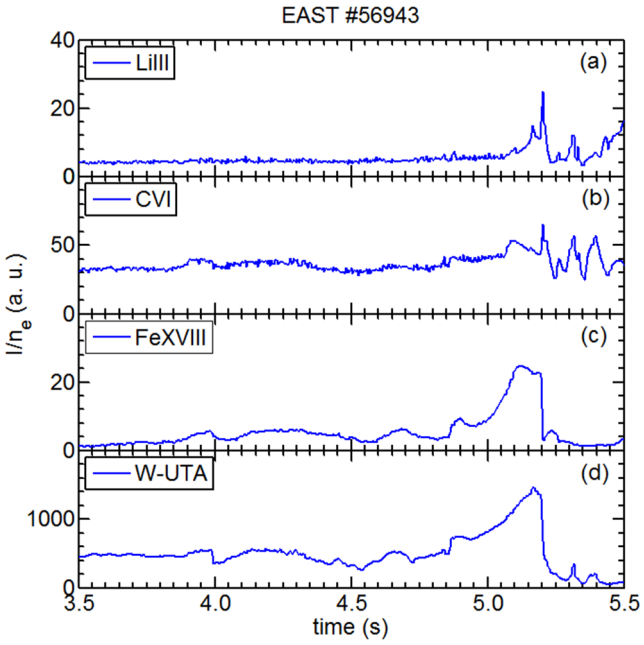

Figure 6. Time evolution of the normalized intensity of (*a*) the LiIII line, (*b*) the CVI line, (*c*) the FeXVIII line, and (*d*) W-UTA (tungsten unresolved transition array in 45–70 A) in shot #56943.

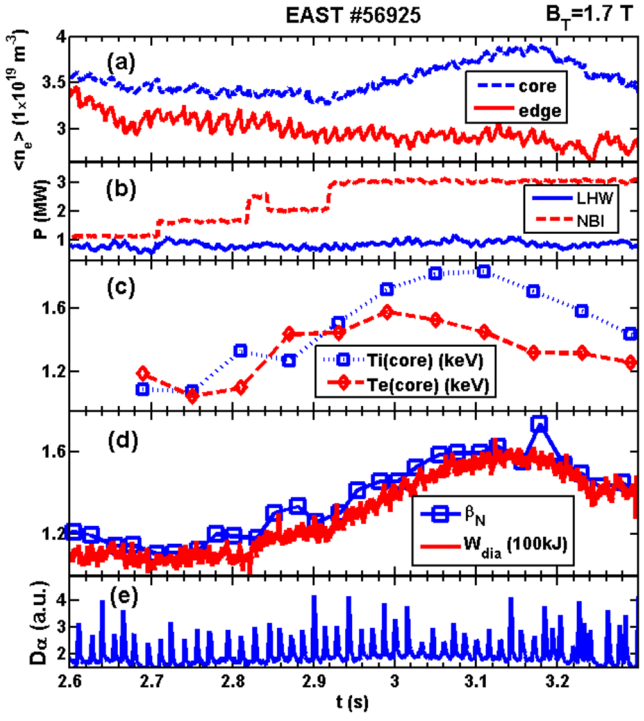

Figure 7. ITB dynamics in EAST. Time traces in the upper figure are (*a*) plasma density (core and edge chord), (*b*) external heating power, (*c*) ion and electron temperature in the core, (*d*) normalized plasma β and plasma stored energy, and (*e*) D_α signal as an indication of an ELM.

EAST high-β_N database, about 35.5% (17 out of 48) of the discharges belong to this category. This observation implies that control of impurities and impurity radiation is a key issue for long-pulse high-β_N operation [27].

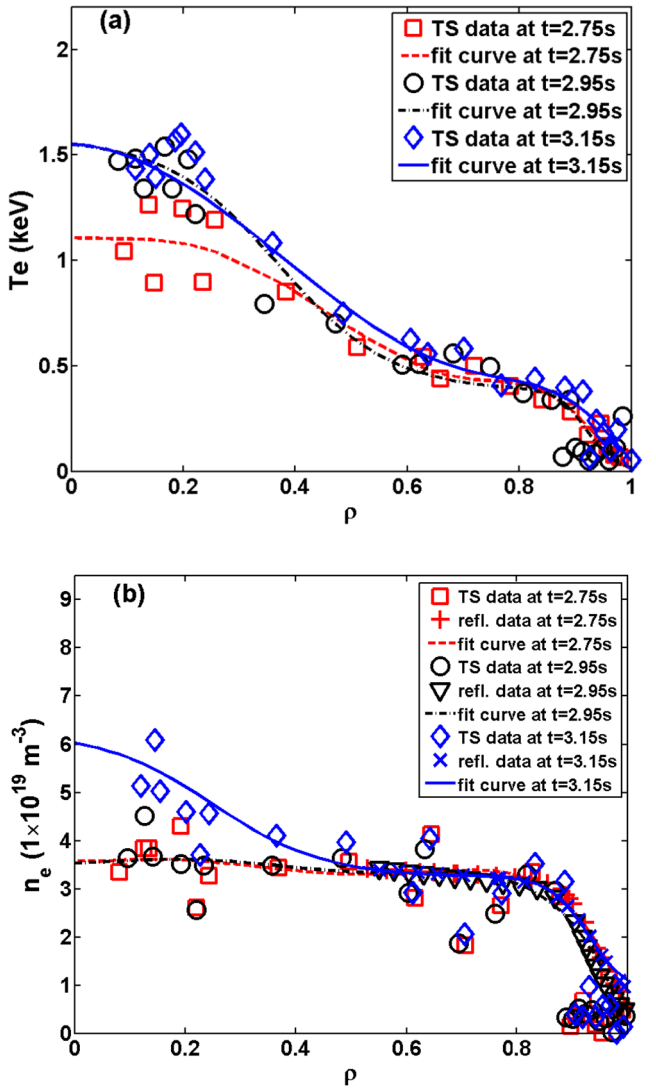

Figure 8. Temperature and density profiles during the ITB dynamics on shot #56925: (*a*) electron temperature profiles and (*b*) electron density profiles.

3.3. ITB dynamics in ELMy H-mode plasmas

In the 2015 campaign, an internal transport barrier (ITB) was observed on EAST. An ITB was observed in 23% (11 out of 48) of the discharges. All these discharges were ELMy H-mode discharges with lower single null configuration. This further improved confinement regime could introduce broader operation space to EAST, benefitting both confinement and long-pulse operation.

One example is presented in figure 7. The plasma current was 450 kA and the toroidal field was 1.7 T in this discharge. A LHW was applied throughout the discharge. The ELMy H mode was established by injection of co-current NBI at $t = 2.4$ s. β_N started to further increase from 1.1 (at $t = 2.82$ s). At $t = 3$ s, the β_N value exceed 1.5 and was sustained for 0.2 s. From $t = 2.7$ s to $t = 3$ s the heating power increased by several steps. This phase was associated with formation of an ITB. In this phase, the core density increased from 3.3×10^{19} m^{-3} to 3.9×10^{19} m^{-3} (a 20% increase). The density peaking

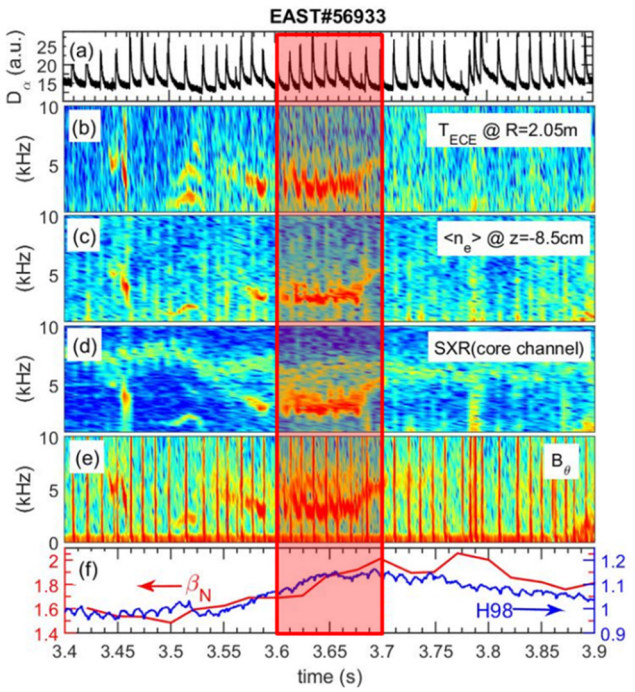

Figure 9. Core MHD ($m/n = 1/1$ fishbone) activities in the ITB phase.

factor increased from 1.25 to 1.5. The core electron temperature increased from 1.1 keV to 1.6 keV (a 45% increase) and the core ion temperature increased from 1.1 keV to 1.8 keV (a 60% increase). The plasma stored energy also increased by 45%. So both electron and ion ITBs were observed. The ITB collapsed at $t = 3.18$ s, associated with the drop in β_N and plasma stored energy.

What is interesting is the time difference in the electron density and temperature of ITB dynamics. The electron density barrier is easier to describe. From the multi-channel line averaged density signal, the edge chord remains and even dropped slightly throughout the phase ($t = 2.82$–3.18 s), while the core chord increased from $t = 2.92$ s. So maintenance of the electron density barrier could be considered from $t = 2.92$ s to $t = 3.18$ s. Further evidence can be found in the density profile [data from Thomson scattering (TS) and reflectometry] presented in figure 8(b). One can see that a temperature barrier exists at $t = 3.15$ s, while there was no barrier at $t = 2.75$ s (figure 8(a)). The profile data at $t = 2.95$ s show that there was a temperature ITB but no density ITB. Additionally, the core temperature started to increase at $t = 2.8$ s, associated with the starting time of the ITB phase ($t = 2.82$ s). These data imply that the formation of the temperature ITB was near 2.82 s. The decay of the ITBs in these three channels showed quite a different behavior. From figures 7(a) and (c), the electron temperature collapsed first, even before $t = 3.15$ s when the TS data were collected. Later, the ion temperature collapsed at $t = 3.1$ s, while the density ITB collapsed at $t = 3.18$ s (together with the collapse of β_N). The detailed reason for the ITB collapse is still under investigation. A more detailed analysis of ITB formation and the power threshold can be found in [28].

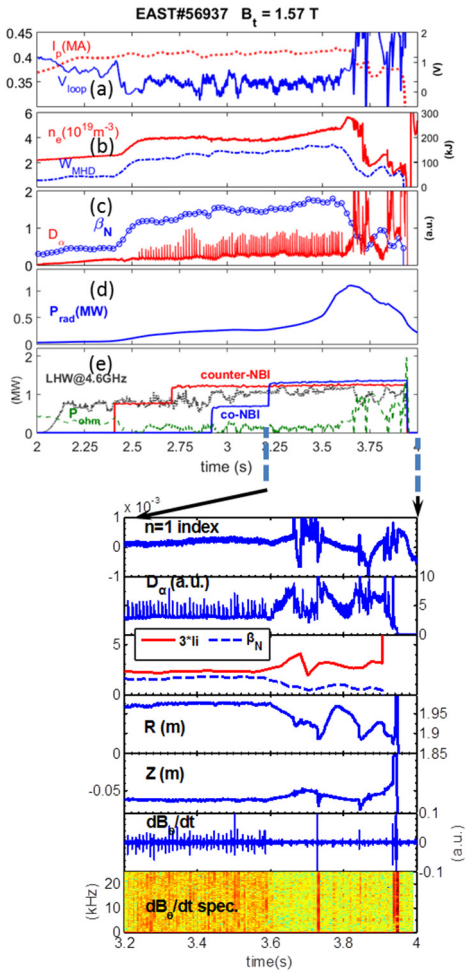

Figure 10. Time traces in the upper figure are (a) plasma and loop voltage, (b) plasma density and stored energy, (c) β_N and the D_α signal as an indication of ELM, (d) the total radiation power, (e) external heating powers and ohmic power. The lower figure shows the time window between 3.2 s and 4 s in more detail, implying the dropout of β_N associated with loss of plasma control.

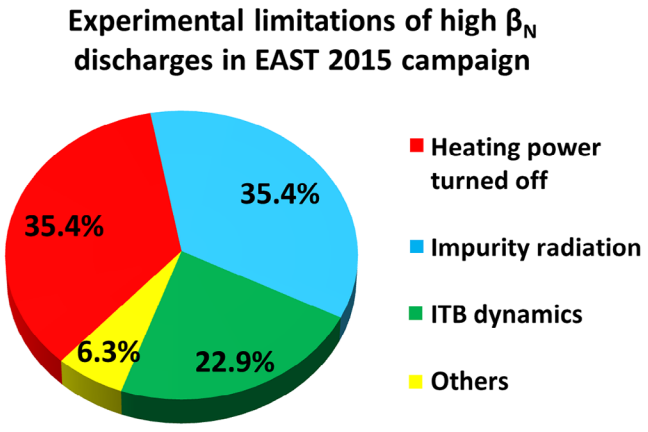

Figure 11. The limitations of high-β_N discharges in the 2015 EAST campaign.

Magnetohydrodynamic (MHD) activities have been studied during the ITB discharge. In another ITB discharge (EAST #56933) in the high-β_N database, sawteeth appeared at $t = 2.7$ s and could be observed on ECE and

SXR signals in the H-mode phase. The reverse surface of the sawteeth indicates that a $q = 1$ surface exists. The sawteeth vanished at $t = 3.5$ s before the ITB phase, which was at $t = 3.54$–3.78 s in figure 9. It is observed that the fishbone mode appears with a frequency of 3–5 kHz for $t = 3.6$–3.7 s during the ITB phase. This mode can be observed on ECE, SXR, FIR and Mirnov coil signals, as shown in figure 9. Typical frequency whistling-down can be confirmed by further wavelet analysis. An $m/n = 1/1$ mode structure was obtained from the wavenumber analysis [29]. This mode indicates that the central safety factor was in the vicinity of 1. From the sawteeth to the fishbone activity, the $q = 1$ surface remained in the plasma. However, due to the fact that the sawteeth disappeared before the formation of the ITB and the appearance of the fishbone during the ITB formation, some change in the safety factor profile is implied. Furthermore, the disappearance of the fishbone indicated another possible change in the safety factor profile. This may also link to the collapse of the ITB ($t = 3.78$ s) shortly afterwards. These analysis needs to be confirmed by more ITB experiments in the future, since there is no safety factor measurement in these discharges.

3.4. The collapse of β_N in ELMy H-mode discharges

There were also several discharges limited by β_N collapse in ELMy H-mode plasmas. As shown in figure 10, the plasma current was 440 kA and the toroidal field was 1.57 T in this discharge. The ELMy H mode was established at $t = 2.45$ s. With a stepwise increase in the NBI power, β_N increased to 1.5. At $t = 3.6$ s, β_N collapsed with the H–L transition. Meanwhile, the plasma lost horizontal and vertical control, as shown in the lower part of figure 10. Before 3.6 s, there was no magnetic perturbation mode on the magnetic probes. At $t = 3.68$ s the $n = 1$ mode was observed on the saddle coil signal and led to the disruption. Because the lower hybrid current drive (LHCD) is applied for ELMy H-mode discharges, which often leads to a broadened current profile, the value of the internal inductance li is only 0.7 before the collapse, as shown in figure 10. During the full heating power phase, β_N approached three times the internal inductance li. However, at the moment of β_N collapse, β_N had still not reached $3li$ but was over $2.5li$. It is not clear whether the collapse corresponded to the no-wall limit which normally is several times li. Such a discharge was one example of discharges that could not be easily categorized and were generally listed as β_N collapse.

4. Summary

In the previous sections the high-β_N (>1.5) database has been introduced and different types of high-β_N (>1.5) discharges have been presented. In section 3.1 the importance of a stable high heating power was indicated. In the database, the failure rate of β_N maintenance due to turning off of the heating power (especially NBI high-voltage breakdown) amounted to 35.4% of all discharges. EAST has improved the NBI system recently and heating power failure could be expected to reduce significantly. In section 3.2 impurity radiation was shown to be one major cause of β_N collapse and even consequent disruptions. Interaction between the plasma and the in-vessel components could be the source of impurities. In 2016, the protection limiter of the LHW antennae was improved in order to mitigate impurity contamination from the limiter. This was found to be practical in recent EAST experiments. In section 3.3 the further confinement improvement regime (ITB) on EAST was discussed. ITB dynamics were described. The reason for β_N collapse in the ITB phase is not yet clear. ITB formation in an ELMy H-mode plasma is a new observation for EAST. An ITB is observed when the sawteeth disappear but with q in the centre still near 1. The related physics study, including the formation, dynamics and collapse, could be another key issue for EAST long-pulse high-β operation in the future.

There are still some discharges that could not be clearly categorized by the mechanism of β_N failure. This needs further study in the future. In general, a brief graph presenting the experimental limitations of high-β_N discharges in EAST could be drawn, as shown in figure 11. The four main mechanisms listed in figure 11 were concluded from the discussions above. These four mechanisms are considered as the key issues for the long-pulse high-β_N (~2) scenario in EAST.

In summary, high-β_N (>1.5) discharges with NBI and 4.6 GHz LHW systems in the 2015 EAST campaign have been studied. The β value increases with increased heating power within a certain range. By studying the drop or collapse of β_N in different typical discharges, four mechanisms limiting the value of β_N have been explored and discussed as key issues governing long-pulse high-β_N discharges in EAST. These include: (1) increasing and sustaining a reliable high heating power; (2) control of impurity radiation during high-power experiments; (3) study of ITB dynamics (formation, development and collapse); and (4) understanding the β_N collapse mechanisms. These key issues need to be further studied and confirmed in future EAST experiments.

Acknowledgments

This work is supported by the National Magnetic Confinement Fusion Program of China with contract nos 2014GB106000, 2014GB106001, 2014GB106002, 2014GB106003, 2014GB106004 and 2014GB106005 and the National Nature Science Foundation of China with contract nos 11505238 and 11675211.

References

[1] Shimada M. *et al* 2007 *Nucl. Fusion* **47** S1
[2] Gormezano C. *et al* 2007 *Nucl. Fusion* **47** S285
[3] Hender T.C. *et al* 2007 *Nucl. Fusion* **47** S128
[4] Kamada Y. *et al* 1999 *Nucl. Fusion* **39** 1845
[5] Ide S. *et al* 2000 *Nucl. Fusion* **40** 445
[6] Gao X. *et al* 2001 *Plasma Phys. Control. Fusion* **43** 1759
[7] Greenfield C.M. *et al* 2003 *Phys. Plasmas* **11** 2616
[8] Murakami M.R. *et al* 2003 *Phys. Rev. Lett.* **90** 255001
[9] Wade M.R. *et al* 2003 *Nucl. Fusion* **43** 634

[10] Litaudon X. *et al* 2002 *Plasma Phys. Control. Fusion* **44** 1057
[11] Fujita T. *et al* 2001 *Phys. Rev. Lett.* **87** 085001
[12] Sakamoto Y. *et al* 2005 *Nucl. Fusion* **45** 574
[13] Shiraiwa S. *et al* 2004 *Phys. Rev. Lett.* **92** 035001
[14] Sauter O. *et al* 2002 *29th EPS Conf. (Montreux, 2002)* P2.087 (www.researchgate.net/publication/37461988)
[15] Suzuki T. *et al* 2004 *Nucl. Fusion* **44** 699
[16] Sips A.C.C. *et al* 2002 *Plasma Phys. Control. Fusion* **44** A151
[17] Sips A.C.C. *et al* 2003 *Fusion Sci. Technol.* **44** 605
[18] Luce T.C. *et al* 2001 *Nucl. Fusion* **44** 1585
[19] Luce T.C. *et al* 2003 *Nucl. Fusion* **43** 321
[20] Li J. *et al* 2013 *Nat. Phys.* **9** 817
[21] Wan B. *et al* 2016 Overview of EAST experiments on the development of high-performance steady-state scenario *Preprint: 2016 IAEA Fusion Energy Conf. (Kyoto, Japan, 17–22 October 2016)* [OV/2-2]
[22] Gao X. *et al* 2015 *Plasma Sci. Technol.* **17** 448
[23] Qian J. *et al* 2016 *Plasma Sci. Technol.* **18** 457
[24] Takenaga H. *et al* 2003 *Nucl. Fusion* **43** 1235
[25] Rice J.E. *et al* 2002 *Nucl. Fusion* **42** 510
[26] Li Y.L. *et al* 2015 *Phys. Plasmas* **22** 022510
[27] Gao X. *et al* 2016 Impurity behavior in high β_N discharges on EAST tokamak *Presented at 6th APTWG Int. Conf. (Seoul, Korea, 21–25 June 2016)*
[28] Yang Y. *et al* 2016 Observation of ITB formation on EAST tokamak *Presented at 6th APTWG Int. Conf. (Seoul, Korea, 21–25 June 2016)*
[29] Xu L.Q. *et al* 2015 *Phys. Plasmas* **22** 122510